5-1-2020

Multiple mineral horizons in layered outcrops at Mawrth Vallis, Mars, signify changing geochemical environments on early Mars

Janice L. Bishop
SETI Institute

Christoph Gross
Freie Universität Berlin

Jacob Danielsen
San Jose State University

Mario Parente
University of Massachusetts Amherst

Scott L. Murchie
Johns Hopkins University Applied Physics Laboratory

See next page for additional authors

Recommended Citation

Janice L. Bishop, Christoph Gross, Jacob Danielsen, Mario Parente, Scott L. Murchie, Briony Horgan, James J. Wray, Christina Viviano, and Frank P. Seelos. "Multiple mineral horizons in layered outcrops at Mawrth Vallis, Mars, signify changing geochemical environments on early Mars" *Icarus* (2020). https://doi.org/10.1016/j.icarus.2020.113634

Authors

Janice L. Bishop, Christoph Gross, Jacob Danielsen, Mario Parente, Scott L. Murchie, Briony Horgan, James J. Wray, Christina Viviano, and Frank P. Seelos

Icarus 341 (2020) 113634

Contents lists available at ScienceDirect

Icarus

journal homepage: www.elsevier.com/locate/icarus

Multiple mineral horizons in layered outcrops at Mawrth Vallis, Mars, signify changing geochemical environments on early Mars

Janice L. Bishop [a,b,*], Christoph Gross [b], Jacob Danielsen [a,c], Mario Parente [d], Scott L. Murchie [e], Briony Horgan [f], James J. Wray [g], Christina Viviano [e], Frank P. Seelos [e]

[a] SETI Institute, Mountain View, CA, United States of America
[b] Freie Universität Berlin, Berlin, Germany
[c] San Jose State University, San Jose, CA, United States of America
[d] University of Massachusetts at Amherst, Amherst, MA, United States of America
[e] Johns Hopkins University Applied Physics Lab, Laurel, MD, United States of America
[f] Purdue University, West Lafayette, IN, United States of America
[g] Georgia Institute of Technology, Atlanta, GA, United States of America

ARTICLE INFO

Keywords:
Mars
Mineralogy
Spectroscopy
Aqueous processes
Salt
Climate

ABSTRACT

Refined calibrations of CRISM images are enabling identification of smaller deposits of unique aqueous materials on Mars that reveal changing environmental conditions at the region surrounding Mawrth Vallis. Through characterization of these clay-sulfate assemblages and their association with the layered, phyllosilicate units of this region, more details of the aqueous geochemical history can be gleaned. A stratigraphy including five distinct mineral horizons is mapped using compositional data from CRISM over CTX and HRSC imagery across 100s of km and from CRISM over HiRISE imagery across 100s of meters. Transitions in mineralogic units were characterized using visible/near-infrared (VNIR) spectral properties and surface morphology. We identified and characterized complex "doublet" type spectral signatures with two bands between 2.2 and 2.3 μm at one stratigraphic horizon. Based on comparisons with terrestrial sites, the spectral "doublet" unit described here may reflect the remnants of a salty, evaporative period that existed on Mars during the transition from formation of Fe-rich phyllosilicates to Al-rich phyllosilicates. Layered outcrops observed at Mawrth Vallis are thicker than in other altered regions of Mars, but may represent processes that were more widespread in wet regions of the planet during its early history. The aqueous geochemical environments supporting the outcrops observed here include: (i) the formation of Fe^{3+}-rich smectites in a warm and wet environment, (ii) overlain by a thin ferrous-bearing clay unit that could be associated with heating or reducing conditions, (iii) followed by a transition to salty and/or acidic alteration phases and sulfates (characterized by the spectral "doublet" shape) in an evaporative setting, (iv) formation of Al-rich phyllosilicates through pedogenesis or acid leaching, and (v) finally persistence of poorly crystalline aluminosilicates marking the end of the warm climate on early Mars. The "doublet" type units described here are likely composed of clay-sulfate assemblages formed in saline, acidic evaporative environments similar to those found in Western Australia and the Atacama desert. Despite the chemically extreme and variable waters present at these terrestrial, saline lake environments, active ecosystems are present; thus, these "doublet" type units may mark exciting areas for continued exploration important to astrobiology on Mars.

1. Introduction

Investigation of phyllosilicate-bearing deposits on Mars provides an opportunity to evaluate aqueous activity and changes in climate. The Mawrth Vallis region lies at the border of the southern highlands and the northern lowlands near 22–25°N and 17–21°W. It is defined by the Mawrth Vallis channel and the ~100-km wide Oyama crater, and has been modified by numerous impact craters and small outflow tributaries, as well as volcanism (e.g., Tanaka et al., 2005; Loizeau et al., 2007; Michalski and Fergason, 2009; Michalski and Bleacher, 2013).

* Corresponding author at: SETI Institute, Mountain View, CA, United States of America.
E-mail address: jbishop@seti.org (J.L. Bishop).

https://doi.org/10.1016/j.icarus.2020.113634
Received 29 June 2019; Received in revised form 19 December 2019; Accepted 9 January 2020
Available online 17 January 2020

Elevation varies from approximately −2700 to −3600 m (e.g., Loizeau et al., 2007) and extensive Fe- and Al-bearing phyllosilicate outcrops were first identified in Mars Express OMEGA (Observatoire pour la Minéralogie, L'Eau, les Glaces et l'Activité) images (Poulet et al., 2005). The ancient phyllosilicate-rich rocks were emplaced ~4.0–3.8 Ga ago (Loizeau et al., 2012b), largely through sedimentary processes (Michalski and Noe Dobrea, 2007; Lowe et al., 2020) involving aqueous alteration of pyroclastic material through processes such as pedogenesis (Bishop et al., 2008b; McKeown et al., 2009; Horgan et al., 2013). This was one of the first regions where Al-rich phyllosilicates were identified stratigraphically above Fe-rich phyllosilicates because of their large spatial occurrence (Poulet et al., 2005; Bishop et al., 2008b); subsequent analyses have shown that Al-phyllosilicates commonly occur over Fe/Mg-phyllosilicates on Mars and may represent widespread pedogenic alteration in warm, aqueous environments with high water/rock ratios (Carter et al., 2015a).

Analysis of hyperspectral visible/near-infrared (VNIR) spectra acquired by the Compact Reconnaissance Imaging Spectrometer for Mars (CRISM) on board the Mars Reconnaissance Orbiter (MRO) has shown thick, complex profiles of phyllosilicates at Mawrth Vallis, consistent with aqueous alteration and active chemistry (e.g., Bishop et al., 2008b; McKeown et al., 2009; Bishop et al., 2013a). These phyllosilicates occur in finely-layered profiles 300 m or more thick (Loizeau et al., 2010). Recent modeling of phyllosilicate formation conditions suggests that these phyllosilicate-rich units could have formed during short-term warm and wet environments in an otherwise cold early Mars (Bishop

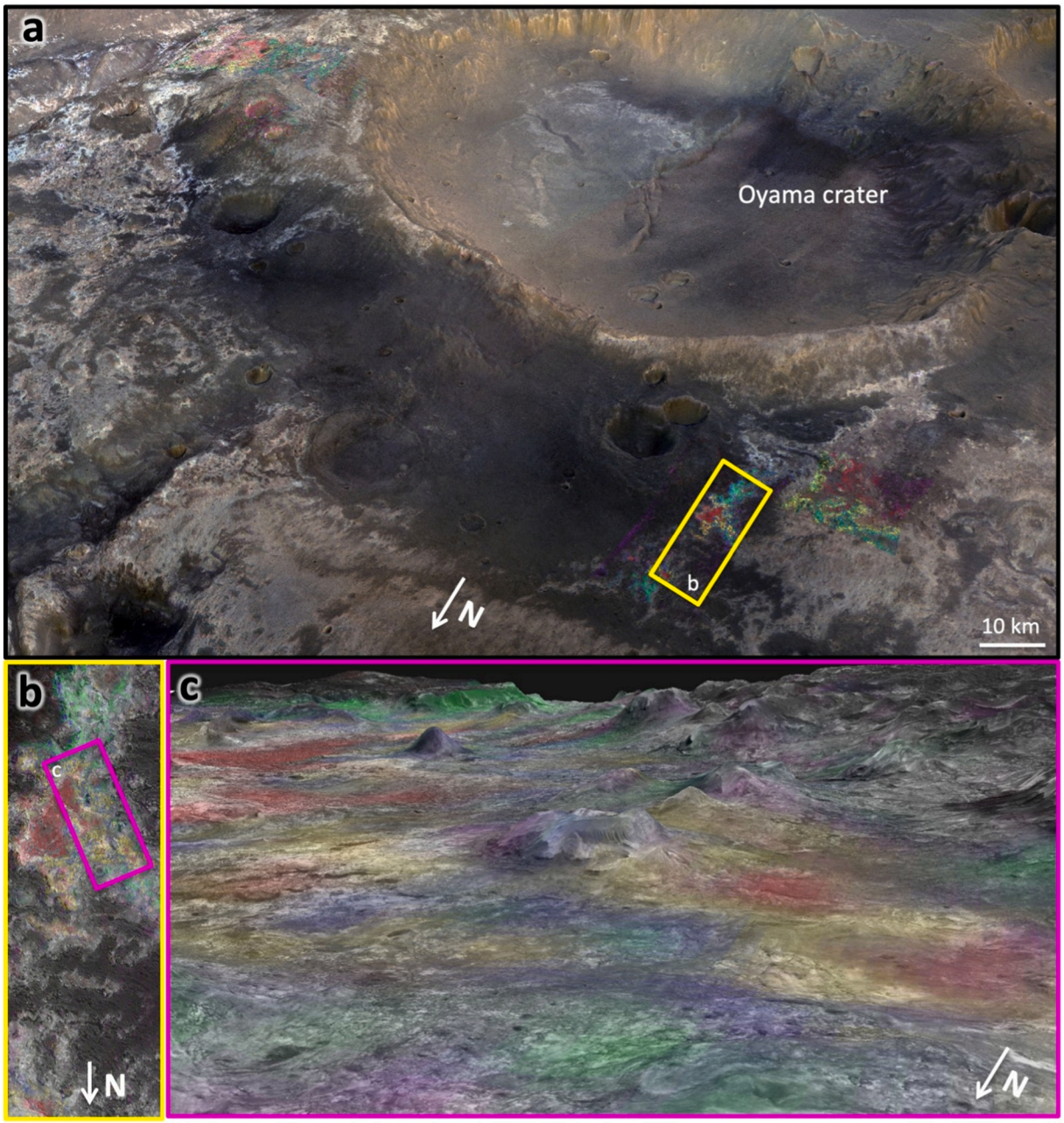

Fig. 1. View of multiple mineral horizons at Mawrth Vallis. a) Oblique view from HRSC mosaic and DTM MC11E with 7-fold vertical exaggeration featuring phyllosilicate-bearing outcrops in CRISM false-color data from images HRL000043EC and FRT0000AA7D in the foreground with parameters BD2290 in red, OLINDEX3 in purple, MIN2250 in yellow, BD2210_2 in blue, and BD2190 in green, b) CRISM false-color data as in (a) draped over HiRISE image PSP_005819_2050 for inset region in (a), and c) HiRISE image PSP_005819_2050 over a HiRISE DTM, draped with CRISM false-color data as in (a) for inset region in (b). (For interpretation of the references to color in this figure legend, the reader is referred to the web version of this article.)

et al., 2018). Because of the altered Noachian rocks, abundant phyllosilicates, changing redox conditions, evidence of habitable conditions, and likely preservation of biosignatures at Mawrth Vallis, this site has been a candidate landing site for many surface missions (e.g., Michalski et al., 2010; Bishop et al., 2013a; Gross et al., 2017; Poulet et al., 2020).

Light-toned phyllosilicate-rich outcrops are visible across the Mawrth Vallis region surrounding Oyama crater and along the main channel (Fig. 1) where exposed through the caprock. This study builds on previous detections of phyllosilicates (Poulet et al., 2005; Bishop et al., 2008b; Wray et al., 2008; McKeown et al., 2009; Michalski and Fergason, 2009; Murchie et al., 2009a; Noe Dobrea et al., 2010; Bishop et al., 2013a; Michalski et al., 2013; Bishop and Rampe, 2016; Bishop et al., 2018), sulfates (Farrand et al., 2009; Wray et al., 2010; Michalski et al., 2013; Farrand et al., 2014), and doublet-type units (Bishop et al., 2013a; Bishop et al., 2016) observed at the Mawrth Vallis region. Most of the aqueous alteration producing these phyllosilicates and sulfates formed before emplacement of the caprock unit about 3.7–3.6 Gya (Loizeau et al., 2012a).

The purpose of this study is to characterize the newly identified "doublet" type units in terms of possible phyllosilicates and sulfates from lab and field studies and provide constraints on their aqueous geochemical history. This work also evaluates the position of the "doublet" unit in the stratigraphy and describes multiple horizons at the study site that are governed by changing environmental conditions or climate.

2. Methods

VNIR spectra from CRISM images (Murchie et al., 2009b) with 18 m/pixel surface resolution for Full Resolution Targeted (FRT) and 36 m/pixel surface resolution for Half Resolution Long (HRL) images were analyzed in this study. Recently processed Map-projected Targeted Reduced Data Record (MTRDR) calibration images (Seelos et al., 2016) were evaluated; these images are processed through a pipeline that includes the standard photometric corrections, a "volcano scan" correction for atmospheric gas absorptions (e.g., McGuire et al., 2009), and a correction for wavelength calibration over time (Morgan et al., 2011). MTRDR images contain spectra joined across the Short (S) and Long (L) wavelength images to span the full 0.4–3.9 μm range, and include improved spectral quality due to empirical corrections for along-track variations in aerosol opacity due to the geometry of the targeted (gimbaled) observations (Seelos, 2011). These images are available at: http://pds-geosciences.wustl.edu/missions/mro/crism.htm. We used the Viviano-Beck et al. (2014) spectral indices for visualizing surface mineralogy for our analyses as they offer more precise separation of features in the range 2.17–2.4 μm than the original Pelkey et al. (2007) parameters. In particular, we used the parameters OLINDEX3, BD2190, BD2210_2, MIN2250, BD2265, and BD2290 for identification of the spectral units in this study. For the 5-color images, we assigned BD2190 to green, BD2210 to blue, MIN2250 to yellow (green and red), OLINDEX3 to purple (red and blue), and BD2290 to red. We overlayed individual, single-colored CRISM tif/tfw pairs for each parameter on the HRSC and HiRISE DTMs in the ArcGIS project, which enables distinguishing each of these five units in distinct colors.

We devised an ad-hoc procedure to distinguish spectra having a band in the region 2.20–2.25 μm versus 2.25–2.30 μm, or both regions. The images were first corrected for artifacts using the column-average-based noise suppression technique described in Parente et al. (2014). Each spectrum is further median-filtered and then fit with a cubic-smoothing spline. A continuum is estimated and removed by division. The identification of the precise position of local minima in the ranges 2.174–2.234 μm and 2.274–2.304 μm is easily obtained on the continuum-removed spline. Locations having bands in either or both of these spectral regions were mapped in order to visualize the spatial occurrence of these components.

3D views of MTRDR images were prepared by overlaying the CRISM false color images of mineral parameters on top of Mars Orbiter Laser Altimeter (MOLA) data at ~120 m surface resolution (Smith et al., 2001) using ENVI software (Harris Geospatial Solutions). ArcGIS software (ESRI) was used to overlay false color CRISM images over MRO High Resolution Imaging Science Experiment (HiRISE) images at ~30 cm/pixel surface resolution (McEwen et al., 2007) with coordinated mosaics of MRO Context (CTX) images at ~6 m/pixel surface resolution (Malin et al., 2007) and Mars Express High Resolution Stereo Camera (HRSC) images at ~10 m surface resolution (Neukum et al., 2004; Gwinner et al., 2016). The HRSC digital terrain model (DTM) has a grid size of 50 m and the HiRISE DTM has a grid size of 1 m. The HiRISE DTM was generated at the University of Arizona using methods developed by Kirk et al. (2008) and McEwen et al. (2010).

CRISM I/F spectra were acquired using ENVI software from regions of interest (ROI) ranging from 3 × 3 to 20 × 20 pixels, depending on the size of the outcrop. Relative I/F spectra were produced to minimize contributions from non-surface sources by ratioing the spectra of the site under investigation to a spectrally neutral region in the image. Some of the larger outcrops with strong spectral contrast did not need to be ratioed; however, all of the spectra presented in this paper were ratioed. Specific details on the xy coordinates of the numerator and denominator spectra and the number of pixels in the ROI are provided in supplementary online content. A 3-point boxcar smooth was applied to most of the CRISM spectra. The "doublet" type spectra in this study are defined as those having two bands in the region 2.20–2.30 μm. Typically, these spectra include one band at 2.20–2.23 μm and the other at 2.25–2.29 μm. In order to characterize these "doublet" type spectra, they are compared with lab spectra of minerals and altered materials. The CRISM images investigated here include: FRT00003BFB, HRL000043EC, FRT0000863E, FRT000089F7, FRT000094F6, FRT0000A425, FRT0000AA7D, FRT0000B141, and FRT0000BB59. The outcrops observed in these images are similar to those observed across the Mawrth Vallis region (e.g., Bishop et al., 2013a; Danielsen et al., 2019).

3. Results

3.1. Identification of five distinct horizons in the clay profile

The stratigraphy of the five mineralogically-distinct horizons investigated here is illustrated in Figs. 1–2. An HRSC oblique color view (Fig. 1a) demonstrates the breadth of light-toned phyllosilicate-rich material at Mawrth Vallis. False color CRISM data overlain on HRSC (Figs. 1a,b) and HiRISE (Figs. 1c, 2b) were assigned to green for the nanophase (np) and/or poorly crystalline aluminosilicates (e.g., allophane) with spectral bands near 1.39–1.40, 1.92–1.93, and 2.19–2.20 μm, blue for Al-rich phyllosilicates (e.g., montmorillonite/halloysite) with spectral bands at 1.40–1.41, 1.91–1.92, and 2.20–2.21 μm, yellow for the "doublet" type unit with spectral bands near 2.20–2.23 and 2.25–2.29 μm, purple for the Fe^{2+}-bearing clay with an increasing slope due to ferrous iron, and red for the nontronite or Fe-Mg-smectite unit with spectral features near 1.41–1.43, 1.91–1.92, 2.28–2.30, and 2.38–2.40 μm. Spectra of the Fe^{2+}-bearing unit are characterized by a steeper slope from ~1 to 2 μm (Bishop et al., 2008b) and they often include a mixture of the lower nontronite features and the upper doublet features; in some cases chamosite-type features are included near 2.25 and 2.37 μm (e.g., Fig. 2c). A model of the stratigraphy illustrates the patchy nature of the "doublet" type unit (Fig. 2a).

Previous analyses illustrated a common stratigraphy of Al-phyllosilicates over ferrous material over Fe/Mg-smectites (Bishop et al., 2013a, 2013b) and amorphous phases over Al-phyllosilicates over Fe/Mg-smectites (Bishop and Rampe, 2016). Here we are adding the spectral "doublet" unit that is found in between the Al-rich phyllosilicate unit and the ferrous clay unit (Fig. 2). Each of these 5 units has distinct spectral signatures (Fig. 2c) and morphologies (Fig. 3). The band centers and relative intensities of the "doublet" features are highly variable (Fig. 4), which is consistent with a system more complex than just

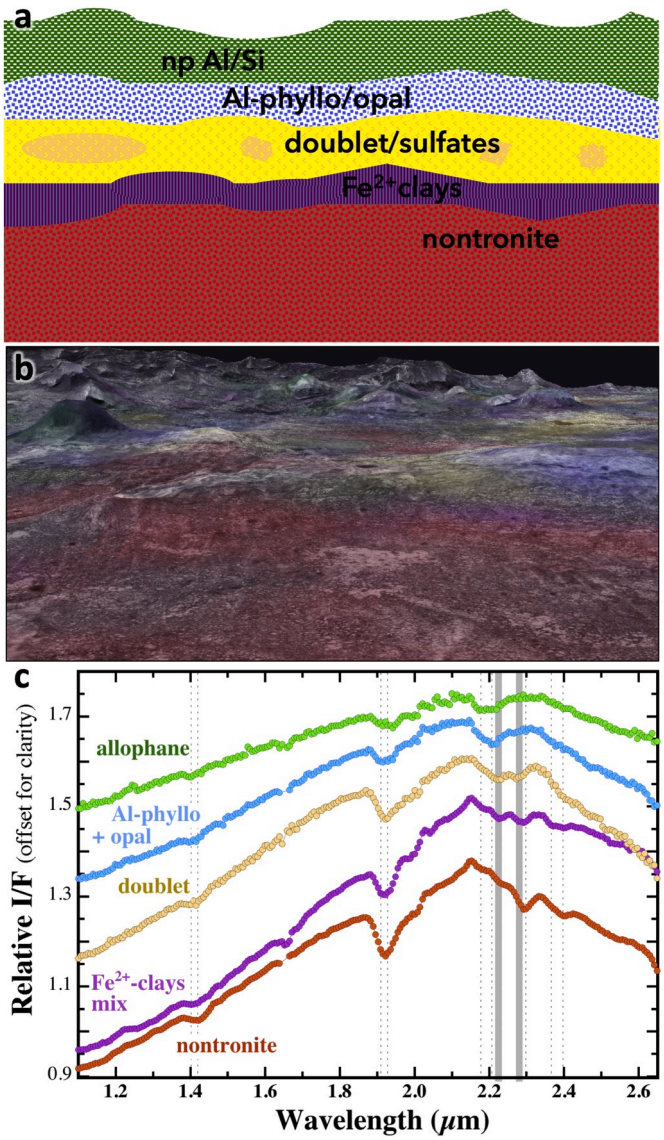

Fig. 2. Stratigraphy of five distinct mineral horizons at Mawrth Vallis. a) Diagram illustrating the nontronite (Fe/Mg-smectite) unit mapped in red at the bottom of the stratigraphic sequence, overlain by ferrous clays in purple, then the spectral "doublet" unit in yellow including sulfates, followed by Al-rich phyllosilicates and opal in blue, and covered by nanophase aluminosilicates (e.g., allophane) in green, b) view of HiRISE stereo terrain model with CRISM false-color data representing these 5 units, and c) spectra representing these 5 stratigraphic units ratioed to nearby spectrally neutral regions to highlight surface features. Grey lines mark features of interest. (For interpretation of the references to color in this figure legend, the reader is referred to the web version of this article.)

mixtures. Most of these spectra were acquired from smaller 3 × 3 or 5 × 5 pixel regions in order to reduce the averaging over multiple surface materials.

3.2. Characterization of the spectral "doublet" unit

Close-up views of the 2.1–2.4 μm range illustrate the variations observed for the "doublet" type outcrops at Mawrth Vallis (Fig. 4b) and the minerals gypsum, jarosite, gibbsite, and butlerite (Fig. 4c). In addition to these minerals, acid treated smectite (ATS) exhibits a doublet feature here (Madejová et al., 1998), as well as some mineral mixtures. Spectra are included in Fig. 4c of a lab mixture of equal weight proportions of jarosite and gypsum and a Painted Desert soil sample containing more jarosite than gypsum (Perrin et al., 2018) that are examples of mixtures having a spectral doublet feature. Spectra of poorly crystalline Fe–SiO_2 phases (Tosca et al., 2008) and some smectites with mixed cations exhibit a broad shoulder feature in this region (not shown) that could also be related to the "doublet" unit.

The spectral features near 2.2–2.3 μm in smectites vary with the type of cation that is connected to OH in the octahedral sheet (e.g., Bishop et al., 1994; Bishop et al., 2008a). The OH combination (stretching plus bending) vibration for the Al_2OH sites in montmorillonite occurs at 2.205–2.212 μm when Al is sufficiently abundant such that nearly all OH groups have two Al cations bound to them (Bishop et al., 2002). This band is broadened or a shoulder develops near 2.23 μm for smectites with some $AlFe^{3+}OH$ sites. Similarly, the OH combination vibration for the $Fe^{3+}{}_2OH$ sites in nontronite occurs at 2.283–2.288 μm when Fe^{3+} is sufficiently abundant that nearly all OH groups have two Fe^{3+} cations bound to them, and a shoulder occurs near 2.23 μm for samples such as SWa-1 ferruginous smectite where some $AlFe^{3+}OH$ sites are present as well as $Fe^{3+}{}_2OH$ sites (Bishop et al., 2002). Sediments containing Al-rich nontronite also include this band near 2.28 μm plus a shoulder at shorter wavelengths (e.g., Bristow et al., 2018). Some regions of Mawrth Vallis do exhibit features (OH combination band and shoulder) that could be consistent with mixed cation smectites; however, the "doublet" type features that are the focus of this investigation include two bands in most cases positioned near 2.20–2.23 and 2.25–2.29 μm.

Three sets of false color views are shown for four CRISM images in Fig. 5 to illustrate the locations of this "doublet" unit in relation to the others featured here. For each set, the false color image at the left illustrates the transition from the allophane-type amorphous material (green) at the top of the clay profile to the montmorillonite/halloysite type unit (blue) below that, and the thick nontronite type unit (red) at the bottom of the profile. The center column highlights variations in the "doublet" type unit (green/yellow/orange) in relation to the nontronite-rich unit (blue). Materials with more jarosite character are mapped in yellow-green and other "doublet" type phases are mapped in yellow-orange tones. The right column represents the materials dominated by Al and Si in blue and those dominated by Fe and Mg in red, while the "doublet" type regions are mapped in white. These image views on the right clearly show the white "doublet" unit in between the lower red nontronite type material and the upper blue Al/Si type materials. Because the "doublet" unit occurs in between the Al/Si-rich upper unit and Fe/Mg-rich lower unit, a logical assumption would be that the "doublet" unit is simply a mixture of these two units. However, the band centers and relative intensities of the two bands vary widely (Figs. 4b, 6). The spectral properties of these "doublet" materials are thus more complex than simple mixtures. Selected spectra from the Mawrth Vallis region are shown in Fig. 6 compared with lab spectra of related phases in order to illustrate the variations among the "doublet" type units and the differences between the "doublet" type phases and the other units present. Because of the variety of spectral features observed for the "doublet" unit, there are likely multiple processes occurring. Some areas may actually be mixtures of phyllosilicates and sulfates or mixtures of two sulfate minerals. More often though this "doublet" unit likely represents a distinct aqueous alteration episode that altered or reprecipitated the other local materials. Analysis of the morphology and location of the "doublet" type unit indicates that this is present above the Fe-rich phases and below the Al-rich phases (Fig. 7) and that the morphologies of these units are consistent with different materials (Figs. 3, 7c).

One explanation for this doublet feature could be that mixtures of the sulfate minerals jarosite and gypsum are present with different relative abundances. These minerals are not typically co-located because jarosite forms in low-pH environments, while gypsum more typically forms in neutral waters. However, they are observed together in some high salt environments such as saline lakes in Western Australia (Benison and Bowen, 2006) and the Atacama desert in Chile (Flahaut et al., 2017). One region of the Painted Desert also features a sulfate hill with co-located jarosite and gypsum (Perrin et al., 2018). VNIR spectra of

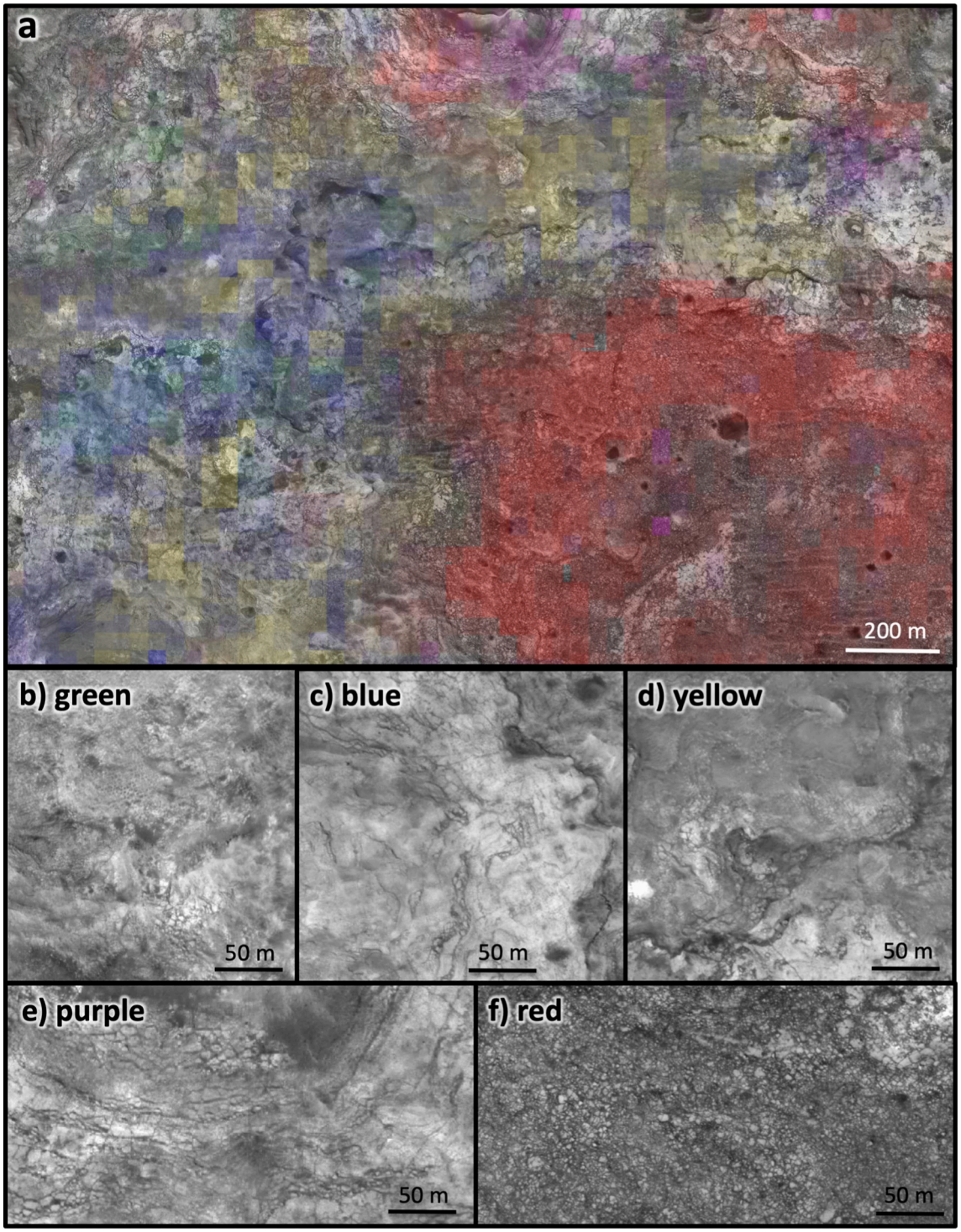

Fig. 3. Surface morphologies of the five mineral horizons from HiRISE image PSP_005819_2050. a) Close-up view of HiRISE stereo terrain model with CRISM false-color data from image HRL000043EC representing these 5 units, b) morphology of poorly crystalline aluminosilicate unit mapped in green, c) morphology of Al-phyllosilicate unit mapped in blue, d) morphology of spectral "doublet" type sulfate-bearing unit mapped in yellow, e) morphology of ferrous clay unit mapped in purple, and f) morphology of Fe/Mg-smectite/nontronite unit mapped in red. (For interpretation of the references to color in this figure legend, the reader is referred to the web version of this article.)

mixtures prepared in the laboratory also include doublets in the 2.2–2.3 μm range for jarosite-gypsum (Perrin et al., 2018), jarosite-nontronite (Usabal and Bishop, 2018), and gypsum-opal (Miura and Bishop, 2018). Another explanation for this "doublet" feature is acid alteration of the Fe-rich smectite unit. Lab experiments with acid-treated smectites (Madejová et al., 1998) and poorly crystalline Fe–SiO_2 phases precipitated in acidic solutions (Tosca et al., 2008) include 2–3 bands in the 2.2–2.3 μm region that vary in band center and band shape depending on the reaction conditions. Hydrothermal alteration of ash near cinder cones, fumeroles, and fresh lava also produces mixtures of jarosite, hydrated silica, and smectites (e.g., Bishop et al., 2005; Bishop et al., 2007; Yant et al., 2017). Because of the variation in band centers

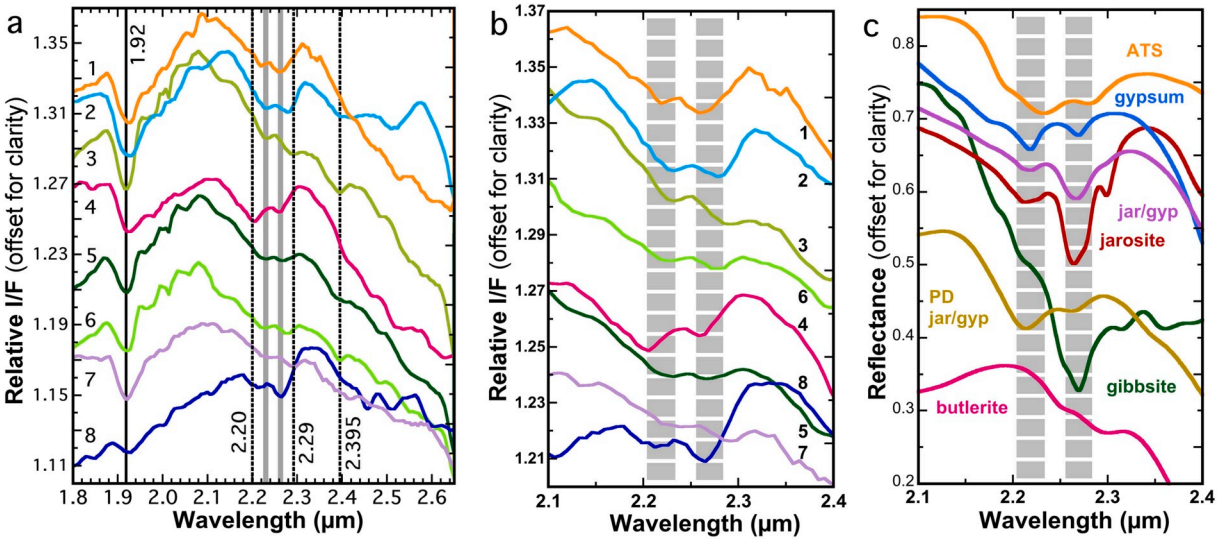

Fig. 4. Spectral character of "doublet" type materials at Mawrth Vallis with two absorption bands occurring between 2.20 and 2.29 μm. a) Selected CRISM relative I/F spectra illustrating this feature from CRISM images (1) FRT0003BFB, (2) FRT0000A425, (3) HRL000043EC, (4) FRT0000863E, (5) HRL000043EC, (6) HRL000043EC, (7) FRT0000AA7D, (8) FRT0000A425. All are ratioed to a spectrally neutral region in the image and the xy coordinates of the numerator and denominator spectra are provided in the supplementary online material. Dark grey lines mark the H_2O band near 1.92 μm (solid line) and OH bands near 2.20, 2.29, and 2.395 μm (dotted lines), while the doublet region near 2.23 and 2.26 μm is marked by light grey lines. Note the variations in H_2O band position and shape as well as other features present in these "doublet" type spectra. b) Same CRISM relative I/F spectra from (a) for the 2.1–2.4 μm region to better illustrate the variations in shape of the "doublet" feature. Note changes in asymmetry of these bands and relative band depths of the bands near 2.20–2.23 μm and near 2.26–2.29 μm. (c) Reflectance spectra of minerals, mixtures, and acid-treated smectite (ATS) that exhibit two bands or a band plus a shoulder feature in this region: ATS (from Madejová et al., 1998), gypsum (from Bishop et al., 2014), jarosite (from Bishop and Murad, 2005), gibbsite (from Bishop collection), butlerite (from Lane et al., 2015), a 50/50 wt% jarosite/gypsum mineral mixture prepared in the lab (jar/gyp) and an orange-colored soil sample from the Painted Desert (PD jar/gyp) that includes ~69 wt% jarosite, ~10 wt% gypsum, ~7 wt% montmorillonite, and ~14 wt% quartz (Perrin et al., 2018).

in addition to changes in relative intensity observed for this "doublet" unit at Mawrth Vallis (Fig. 4c), this unit is attributed to a complex suite of materials rather than a simple mixture. These "doublet" features are consistent with mixtures of Ca sulfates, OH-bearing sulfates and clays, or acid alteration of clays. Thus, this unit likely represents a time period where salty, evaporative environments existed. Saline lakes (e.g., Benison and Bowen, 2006) or salars (e.g., Flahaut et al., 2017) exhibit highly variable mineralogy within tens or hundreds of meters that is consistent with the spectral variations observed for this "doublet" unit at Mawrth Vallis. These salty evaporite regions also represent a range of acidic to mildly acidic to neutral waters. The presence of saline and/or acidic waters could have posed challenges for the evolution of life on early Mars; however, shallow, saline ponds on Earth are enriched with abundant microbial communities (e.g., Benison et al., 2008; Conner and Benison, 2013; Johnson et al., 2015; Benison, 2019; Johnson et al., 2020).

In order to evaluate the "doublet" type unit in more detail, we investigated the tiny outcrops containing potential jarosite-bearing units (Danielsen and Bishop, 2018). CRISM spectra in Fig. 6 attributed to jarosite include bands at 1.47, 1.86 and 2.27 μm (Bishop and Murad, 2005) and are found in several tiny outcrops throughout Mawrth Vallis (Bishop et al., 2016; Danielsen and Bishop, 2018; Usabal et al., 2019). Spectra of jarosite also include a shoulder or weak band near 2.22–2.23 μm. Many of the doublet-type spectra have bands near 2.22–2.23 and 2.26–2.27 μm that are roughly similar to the positions of the jarosite bands, although the relative intensity is inconsistent with jarosite, and other diagnostic jarosite features are missing (e.g., Farrand et al., 2009). However, similar acid-alteration processes are likely responsible for the formation of the doublet-type material and jarosite. Investigation of the sites where jarosite features (1.86, 2.22, and 2.27 μm) are observed and where "doublet" type features are observed shows that they occur in neighboring deposits. The small occurrences of jarosite may indicate localities where acidic conditions persisted longer, thus enabling its formation. Analysis of jarosite mixtures indicate that the 1.86 μm band is only present in systems that contain more jarosite than other sulfate or clay minerals (Perrin et al., 2018; Usabal et al., 2018).

Spectra of the Ca sulfates bassanite and gypsum (Bishop et al., 2014) also contain a doublet near 2.22 and 2.26 μm, similar to jarosite features and a band near 1.75 μm, similar to that of alunite (Bishop and Murad, 2005). Thus, mixtures of these sulfates can be difficult to distinguish. Bassanite was identified previously in small outcrops in at least one part of the Mawrth Vallis region (Wray et al., 2010); thus Ca sulfates could be present in other forms as well. Additional detailed studies are needed to characterize the specific forms of this "doublet" type unit. Investigations to date indicate variations in the shape and character of this "doublet" signature within single CRISM images, while similar types of features are noted in the northern, eastern, and southern parts of this region.

3.3. Characterization of the ferrous spectral unit

Just above the thick nontronite type unit in many locations throughout Mawrth Vallis is a thin horizon containing weaker Fe/Mg-smectite features and a positive slope from ~1 to 1.8 μm that is characteristic of bands due to electronic excitations in ferrous materials (e.g., Burns, 1993). This enhanced positive slope is caused by a broad band arising from an Fe^{2+}-Fe^{3+} charge transfer transition in phyllosilicates (e.g., Faye, 1968; Anderson and Stucki, 1979; Lear and Stucki, 1987). Typically, this increase in the ferrous signature is observed at the top of the nontronite unit where both a positive slope from ~1 to 1.8 μm and a nontronite band near 2.29 μm are observed for only a couple of pixels in the CRISM scene (40–60 m), then the nontronite band disappears further up the stratigraphic column. In some cases, only the ferrous slope is present, while in other cases, bands characteristic of ferrous clays are present and in others the ferrous slope is combined with the "doublet" type features, indicating a mixture of the ferrous material with the "doublet" type unit above it.

This Fe^{2+}-bearing unit could be a mixture of nontronite with ferrous clays such as glauconite (Fe^{2+}Mg-mica), chamosite (Fe^{2+}-rich chlorite

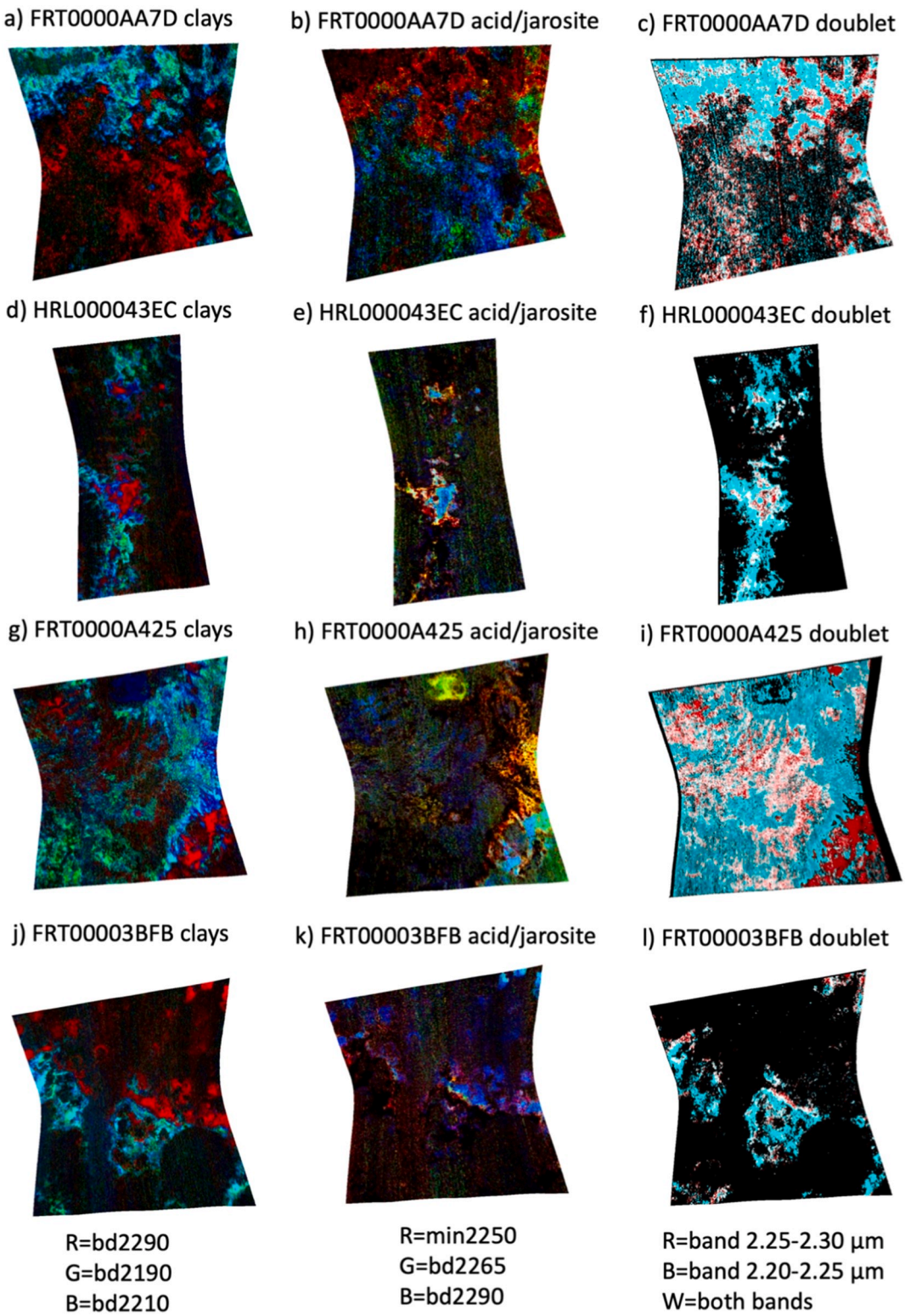

Fig. 5. Views of CRISM image parameter maps illustrating different mineral units in the stratigraphy. Shown in the left column (a, d, g, j) are maps of Fe/Mg-smectite in red, Al-phyllosilicatess in blue, and poorly crystalline aluminosilicates in green. The spectral "doublet" type material is shown in yellow/orange in the center column (b, e, h, k) and in white in the right column (c, f, i, l) using two different sets of parameters. For panels c, f, i, and l, locations where a minimum was identified in the range 2.174–2.234 µm are displayed in cyan, locations where a minimum was identified in the range 2.274–2.304 µm are marked in red, and locations where a doublet feature is present with minima in both ranges are shown in white. (For interpretation of the references to color in this figure legend, the reader is referred to the web version of this article.)

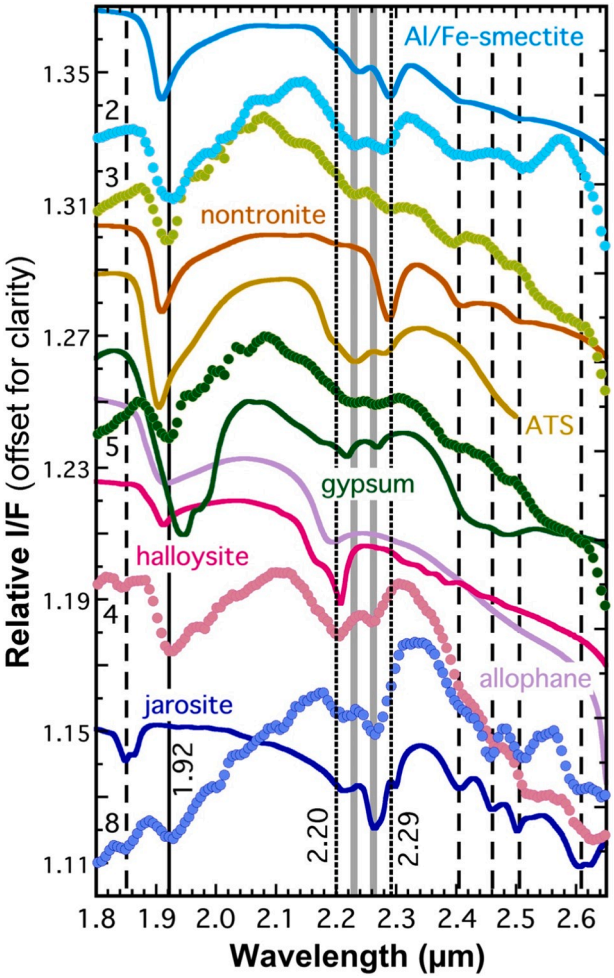

Fig. 6. Selected CRISM spectra from Fig. 4a compared to reflectance spectra of minerals. The lab spectra are labeled with the mineral names and the CRISM spectra have numbers indicating the image where they were collected: (2) FRT0000A425, (3) HRL000043EC, (4) FRT0000863E, (5) HRL000043EC, (8) FRT0000A425. Dashed lines mark features found in jarosite spectra that are strongest in spectrum 8 and partially present in spectrum 4. Both of these spectra include features near 1.92 and 2.20 μm that are most consistent with allophane but could also be due to halloysite. The solid line at 1.92 μm is due to the H_2O combination (stretch + bend) band and the dotted lines are due to the OH combination band for Si-OH or Al-OH at 2.20 μm and for Fe-OH at 2.29 μm. Spectrum 5 includes broad doublet features centered near 2.23 and 2.27 μm that are most similar to a mixture containing gypsum. Spectra 2 and 3 have narrower features near 2.23 and 2.28–2.29 μm and are most similar to acid-treated Fe-smectite. The light grey lines mark the doublet bands near 2.22–2.24 and 2.25–2.27 μm.

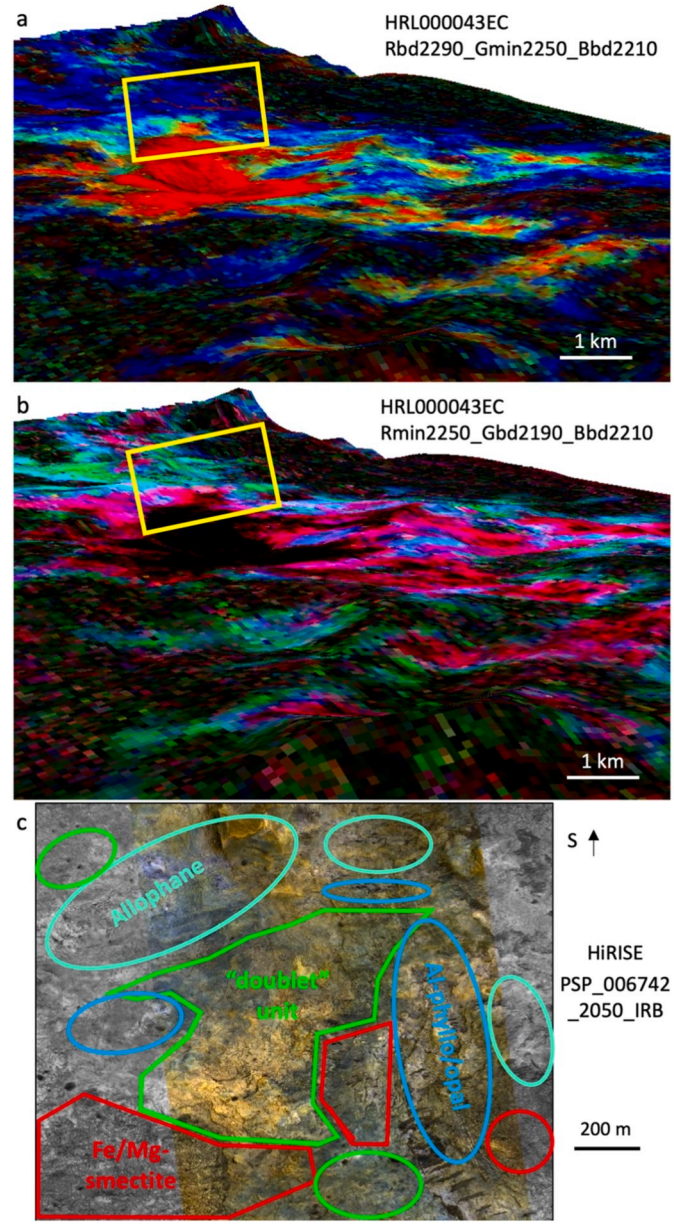

Fig. 7. Expanded views of spectral "doublet" type units. a) 3D views of CRISM image HRL000043EC over MOLA with 5× vertical exaggeration and parameters BD2290 in red, MIN2250 in green, and BD2210_2 in blue, b) 3D views of the same image with parameters MIN2250 in red, in BD2190 green, and BD2210_2 in blue, and c) approximate outlines of compositional units determined by CRISM marked on HiRISE image PSP_006742_2050_IRB. (For interpretation of the references to color in this figure legend, the reader is referred to the web version of this article.)

with some Mg) and celadonite (Mg-rich chlorite with some Fe^{2+}), or it could be a reduced form of nontronite (e.g., Lear and Stucki, 1987; Stucki, 2006; Chemtob et al., 2015). Reduction of Fe^{3+} in nontronite also causes deprotonation of the OH bound to octahedral cations and decreases the intensity of the OH spectral features (Manceau et al., 2000; Fialips et al., 2002). Mixtures of nontronite and ferrous clays or other ferrous minerals also exhibit nonlinear changes in the spectral features, where small amounts of ferrous minerals produced a prominent effect on the mixture spectra (Saper and Bishop, 2011; Bishop et al., 2013b). Thus, an Fe^{2+}-bearing phyllosilicate could be mixed with the lower nontronite or upper "doublet" unit, but not be a major component of this unit and still contribute an increasing slope from ~1 to 1.8 μm. Studies of nontronites heated to 300 °C produced partially irreversible formation of Fe^{2+} species with an upward slope in reflectance spectra from ~1 to 1.8 μm (Morris et al., 2009). These experiments indicate that alteration due to a heating event such as impacts on Mars could be converting a small portion of the Fe^{3+} to Fe^{2+} at the surface of the Fe/Mg-smectite boundary. This would change the spectral properties of the material, but not greatly change the bulk properties of the unit. A ferrous phase could also have been formed due to a redox process when the upper salty, sulfate, and/or Al/Si-rich units formed, then intermixed with each of the phyllosilicate units near their boundary.

A change from a lower Fe^{3+} to an upper Fe^{2+} unit in the stratigraphy is rather unusual and implies that the ferric smectite was present first and then altered to form a ferrous-bearing material. Redox experiments on Fe-rich phyllosilicates in the laboratory have shown that Fe^{3+} in phyllosilicate structures can be reduced via chemical or biological

processes (e.g., Stucki, 2006; Dong et al., 2009); however, microbial reduction is a common process to convert Fe^{3+} to Fe^{2+} in clay minerals (e.g., Dong et al., 2009, and references therein). Anaerobic microbes facilitate these reactions in soils, sediments, and hydrothermal environments on Earth, and smectites (e.g., montmorillonite, nontronite) have been found to provide the highest reduction rates, which was attributed to their expandable layer structures (Stucki et al., 1987; Gates et al., 1998; Dong et al., 2003; Stucki, 2006; Jaisi et al., 2007; Dong et al., 2009). Redox gradients and chemical disequilibria can provide sources of energy for microbes and could be an indicator of habitable environments (Bishop et al., 2013a; Horgan et al., 2015; Bishop, 2018).

3.4. Relationships between mineralogy and climate

The 100–200 m thick deposit of Fe^{3+}/Mg-smectite plus ferric oxide-bearing phases likely occurred in a neutral to slightly basic aqueous environment. In regions such as Mawrth Vallis, where this smectite is not accompanied by high temperature minerals and sedimentary features are observed, this Fe^{3+}-rich smectite likely formed in short-term (tens to 100s of thousands of years), warm (5–10 °C mean annual temperature with seasonal highs up to 20–30 °C) and wet surface environments during the Noachian with rain and leaching of the basalt (Bishop et al., 2018). As described above, alteration of the Fe^{3+}/Mg-smectite unit to produce some Fe^{2+} in the phyllosilicate at the surface of this unit could be an indicator of heating due to impacts, volcanism or magmatic processes, of redox reactions taking place in reduced fluids, or biologic activity. If the ferrous clays formed due to reduction and dehydration through heating, then there was likely an extended period of dry climate during this time. If the ferrous clays formed due to redox reactions then the surface of the 100–200 m thick Fe^{3+}-rich smectite deposit must have been wet (e.g., Bishop et al., 2013a). This could have been achieved in a cold, moist environment with transient liquid water. A fresh supply of Fe^{2+}-bearing volcanic ash could also have been deposited on top of the lower Fe^{3+}-rich smectite unit in an environment with limited water that was too cold for smectite formation. Alternatively, fresh Fe^{2+}-bearing ash soaked in warm, low-pH waters would have supported formation of ferrous clays rather than nontronite (e.g., Chevrier et al., 2007).

The Mawrth Vallis clay-bearing stratigraphy contains the spectral "doublet" material with infrequent, small pockets of jarosite in a thin unit above the ferrous clays. The variable nature of the thickness and composition of the "doublet" type unit implies changing conditions across Mawrth Vallis to produce mixtures of sulfates and clay minerals and acid alteration of the Fe^{3+}-rich smectite unit. This is consistent with an evaporative (e.g., Benison and Bowen, 2006) or hydrothermal (e.g., Bishop et al., 2005) environment. Shallow, saline pools would be easier to explain on Mars at the end of the Noachian and beginning of the Hesperian period because liquid water was likely less stable on the surface of the planet at this time (e.g., Fassett and Head, 2008; Bishop et al., 2018) and there is no evidence of volcanic activity near Mawrth Vallis (Robbins et al., 2011). This "doublet" unit is then covered by the Al-rich phyllosilicate unit. The transition from ferrous clays to salty/sulfate/clay mixtures to Al-phyllosilicates could be explained by aqueous alteration in acidic waters. This was suggested to describe the co-occurrence of jarosite and alunite with Al-rich phyllosilicates in several locations across Mars (Ehlmann and Dundar, 2015). Related "doublet" type features attributed to mixtures of jarosite and clays have been identified at Ius Chasma (Roach et al., 2010; Flahaut et al., 2014) and Noctis Labyrinthus (Weitz et al., 2011). A change from near-neutral waters supporting formation of Fe^{3+}-rich smectite to a drier epoch with occasional acidic waters could explain the observed stratigraphy at Mawrth Vallis. Because the same trend in mineral horizons is observed across thousands of km, the aqueous processes occurring there must have been wide-spread rather than isolated. These alteration episodes occurred at the surface and the rocks have not been significantly modified since then by deep burial or high water activity.

Finally, covering the surface of the clay-rich stratigraphy across Mawrth Vallis is a unit dominated by poorly crystalline, nanophase and amorphous materials such as allophane and imogolite (Bishop and Rampe, 2016). Formation of allophane and imogolite from volcanic glass is favored over smectite clay formation in either low water/rock ratio environments at moderate temperatures or cold climates with high water/rock ratios (Chamley, 1989; Parfitt, 2009; Rasmussen et al., 2010). Other Fe oxide-bearing nanophase and poorly crystalline phases such as ferrihydrite, schwertmannite, and akaganéite have been identified on Mars (Poulet et al., 2008; Carter et al., 2015b) and could have also formed in cooler environments that did not favor formation of crystalline Fe oxides/hydroxides (e.g., Bishop and Murad, 2002; Cornell and Schwertmann, 2003). Thus, the presence of abundant nanophase aluminosilicates without phyllosilicates could mark the end of the warm and wet surface conditions supporting smectite formation (Bishop et al., 2018).

The "doublet" type clay-sulfate assemblages identified in this study are consistent with precipitates and sediments from saline lake environments described previously (e.g., Benison and LaClair, 2003; Benison and Bowen, 2006; Flahaut et al., 2017; Benison, 2019) and may be related to the acid saline environment at Eagle crater, Meridiani, where gypsum- and jarosite-bearing sediments were identified (Squyres et al., 2004). The saline, acid brine lakes in Western Australia and Chile are among the most chemically extreme environments on Earth and host many diverse ecosystems of extremophiles (e.g., Warren-Rhodes et al., 2007; Mormile et al., 2009; Wierzchos et al., 2011; Johnson et al., 2015; Johnson et al., 2020). The water chemistry of these acid lakes in Western Australia fluctuates with flooding and evaporation, producing acidity levels measured at ~1–7 pH and salinities as high as 32% dissolved solids (Benison et al., 2007; Bowen and Benison, 2009). Minerals in these acid lake environments trap organic materials and microorganisms and preserve them over geologically long periods of time (Benison, 2019). Thus, continued investigation of these clay-sulfate assemblages on Mars may provide information to help constrain environments that could have preserved ecosystems if they in fact developed on Mars.

4. Summary

This study describes five distinct mineral horizons observed at Mawrth Vallis in the light-toned, layered units: Fe^{3+}/Mg-smectite, ferrous clays, spectral "doublet" materials, Al-phyllosilicates, and np-aluminosilicates. These layered outcrops observed at Mawrth Vallis are thicker than in other regions of Mars, but may represent processes that took place on a wider scale across Mars during the Noachian time period. Observations at Mawrth Vallis are consistent with the formation of Fe^{3+}-rich smectites in a warm and wet neutral environment, a transition to alteration in acidic waters during a period of evaporative settings with wet/dry cycling, crystallization of Al-rich phyllosilicates through pedogenesis or leaching in warm, acidic waters, followed by colder conditions where the persistence of np-aluminosilicates mark the end of the warm and wet clay-forming climate on Mars. Poorly crystalline materials including allophane, imogolite, ferrihydrite, akaganéite, and schwertmannite would be stable long-term on Mars in the absence of liquid water, but would all alter to form crystalline minerals in warm and wet environments. Because these poorly crystalline phases are observed at the top of the clay stratigraphy at Mawrth Vallis, these signal a long-term dry and cold climate. The layered clay-bearing outcrops at Mawrth Vallis are draped by np-aluminosilicates and covered by caprock. This stratigraphy is observed today where the surface has been eroded.

The layered, light-toned phyllosilicate-rich outcrops at Mawrth Vallis are indicators of changing chemistry that could record an ancient active chemical environment supportive of habitable conditions and would also be able to preserve evidence of ecosystems, if present on ancient Mars, over geologic timescales. Alteration of the Fe^{3+}/Mg-smectite unit to produce some Fe^{2+} in the phyllosilicate at the surface of this unit could be an indicator of heating due to impacts, of redox

reactions taking place in reduced fluids, or biologic activity. Small outcrops of Ca-sulfates, jarosite and alunite are present in pockets between the thick, lower Fe/Mg-smectite unit and the upper Al-phyllosilicate unit. A few isolated regions exhibit spectral properties most consistent with these sulfates, while most occurrences are mixtures with phyllosilicates or hydrated silica. Comparison with terrestrial outcrops containing Ca-sulfates, jarosite, Al-phyllosilicates, and silica/opal suggests that these acidic or salty units at Mawrth Vallis formed in evaporative environments. Alteration in saline and acidic waters could have posed challenges for life, if present, on early Mars; however, such chemically extreme environments on Earth in Western Australia and the Atacama desert contain active ecosystems, indicating that life could have been possible as well in the clay-sulfate assemblages of the martian "doublet" unit outcrops described here.

Acknowledgements

The authors are grateful to the MRO and Mars Express teams that enabled acquiring and processing images from the CRISM, CTX, HiRISE, and HRSC instruments used in this study. We also thank Aaron Kilgallon, Sarah Sutton, and Matt Chojnacki for producing our HiRISE DTM at the University of Arizona. Helpful discussions with B. Ehlmann, editorial suggestions from J. Johnson, and input from two anonymous reviewers improved this paper. Support from NASA's Mars Data Analysis Program (grant #15AM47) and the NASA Astrobiology Institute (grant #15BB01) are much appreciated. CG was supported by the German Space Agency (DLR Bonn), grant 50QM1702 (HRSC on Mars Express), on behalf of the Federal Ministry for Economic Affairs and Energy.

Appendix A. Supplementary data

Supplementary data to this article can be found online at https://doi.org/10.1016/j.icarus.2020.113634.

References

Anderson, W.I., Stucki, J.W., 1979. Effect of structural Fe2+ on visible absorption spectra of nontronite suspensions. In: Mortland, M.M., Farmer, V.C. (Eds.), Developments in Sedimentology. Proceedings of the VI International Clay Conference 1978. Elsevier, Amsterdam, pp. 75–83.
Benison, K.C., 2019. How to search for life in martian chemical sediments and their fluid and solid inclusions using petrographic and spectroscopic methods. Frontiers in Environmental Science 7. https://doi.org/10.3389/fenvs.2019.00108.
Benison, K.C., Bowen, B.B., 2006. Acid saline lake systems give clues about past environments and the search for life on Mars. Icarus 183, 225–229.
Benison, K.C., LaClair, D.A., 2003. Modern and ancient extremely acid saline deposits: terrestrial analogs for martian environments. Astrobiology 3, 609–618.
Benison, K.C., Bowen, B.B., Oboh-Ikuenobe, F.E., Jagnieckl, E.A., LaClair, D.A., Story, S. L., Mormile, M.R., Hong, B.-Y., 2007. Sedimentology of acid saline lakes in southern Western Australia: newly described processes and products of an extreme environment. J. Sediment. Res. 77, 366–388.
Benison, K.C., Jagniecki, E.A., Edwards, T.B., Mormile, M.R., Storrie-Lombardi, M.C., 2008. "Hairy blobs:" microbial suspects preserved in modern and ancient extremely acid lake evaporites. Astrobiology 8, 807–821.
Bishop, J.L., 2018. Chapter 3: remote detection of phyllosilicates on Mars and implications for climate and habitability. In: Cabrol, N.A., Grin, E.A. (Eds.), From Habitability to Life on Mars. Elsevier, pp. 37–75.
Bishop, J.L., Murad, E., 2002. Spectroscopic and geochemical analyses of ferrihydrite from springs in Iceland and applications to Mars. In: Smellie, J.L., Chapman, M.G. (Eds.), Volcano-Ice Interactions on Earth and Mars, Geological Society, Special Publication No. 202, pp. 357–370 (London).
Bishop, J.L., Murad, E., 2005. The visible and infrared spectral properties of jarosite and alunite. Am. Mineral. 90, 1100–1107.
Bishop, J.L., Rampe, E.B., 2016. Evidence for a changing martian climate from the mineralogy at Mawrth Vallis. Earth and Planetary Sci. Lett. 448, 42–48.
Bishop, J.L., Pieters, C.M., Edwards, J.O., 1994. Infrared spectroscopic analyses on the nature of water in montmorillonite. Clay Clay Miner. 42, 702–716.
Bishop, J.L., Madeová, J., Komadel, P., Fröschl, H., 2002. The influence of structural Fe, Al and Mg on the infrared OH bands in spectra of dioctahedral smectites. Clay Miner. 37, 607–616.
Bishop, J.L., Schiffman, P., Lane, M.D., Dyar, M.D., 2005. Solfataric alteration in Hawaii as a mechanism for formation of the sulfates observed on Mars by OMEGA and the MER instruments. In: 36th Lunar Planet. Sci. Conf. Lunar Planet. Inst, Houston (Abstract #1456).
Bishop, J.L., Schiffman, P., Murad, E., Dyar, M.D., Drief, A., Lane, M.D., 2007. Characterization of alteration products in tephra from Haleakala, Maui: a visible-infrared spectroscopy, Mössbauer spectroscopy, XRD, EPMA and TEM study. Clay Clay Miner. 55, 1–17.
Bishop, J.L., Lane, M.D., Dyar, M.D., Brown, A.J., 2008a. Reflectance and emission spectroscopy study of four groups of phyllosilicates: smectites, kaolinite-serpentines, chlorites and micas. Clay Miner. 43, 35–54.
Bishop, J.L., Noe Dobrea, E.Z., McKeown, N.K., Parente, M., Ehlmann, B.L., Michalski, J. R., Milliken, R.E., Poulet, F., Swayze, G.A., Mustard, J.F., Murchie, S.L., Bibring, J.-P., 2008b. Phyllosilicate diversity and past aqueous activity revealed at Mawrth Vallis, Mars. Science 321, 830–833. https://doi.org/10.1126/science.1159699.
Bishop, J.L., Loizeau, D., McKeown, N.K., Saper, L., Dyar, M.D., Des Marais, D., Parente, M., Murchie, S.L., 2013a. What the ancient phyllosilicates at Mawrth Vallis can tell us about possible habitability on early Mars. Planetary and Space Science 86, 130–149.
Bishop, J.L., Perry, K.A., Dyar, M.D., Bristow, T.F., Blake, D.F., Brown, A.J., Peel, S.E., 2013b. Coordinated spectral and XRD analyses of magnesite-nontronite-forsterite mixtures and implications for carbonates on Mars. J. Geophys. Res. 118, 635–650.
Bishop, J.L., Lane, M.D., Dyar, M.D., King, S.J., Brown, A.J., Swayze, G., 2014. Spectral properties of Ca-sulfates: gypsum, bassanite and anhydrite. Am. Mineral. 99, 2105–2115.
Bishop, J.L., Gross, C., Rampe, E.B., Wray, J.J., Parente, M., Horgan, B., Loizeau, D., Viviano-Beck, C.E., Clark, R.N., Seelos, F.P., Ehlmann, B.L., Murchie, S.L., 2016. Mineralogy of layered outcrops at Mawrth Vallis and implications for early aqueous geochemistry on Mars. In: 47th Lunar Planet Sci. Conf (Abstract #1332).
Bishop, J.L., Fairén, A.G., Michalski, J.R., Gago-Duport, L., Baker, L.L., Velbel, M.A., Gross, C., Rampe, E.B., 2018. Surface clay formation during short-term warmer and wetter conditions on a largely cold ancient Mars. Nature Astronomy 2, 206–213.
Bowen, B.B., Benison, K.C., 2009. Geochemical characteristics of naturally acid and alkaline saline lakes in southern Western Australia. Appl. Geochem. 24, 268–284.
Bristow, T.F., et al., 2018. Clay mineral diversity and abundance in sedimentary rocks of Gale crater, Mars. Sci. Adv. 4 https://doi.org/10.1126/sciadv.aar3330.
Burns, R.G., 1993. Mineralogical Applications of Crystal Field Theory. Cambridge University Press, Cambridge, UK.
Carter, J., Loizeau, D., Mangold, N., Poulet, F., Bibring, J.-P., 2015a. Widespread surface weathering on early Mars: a case for a warmer and wetter climate. Icarus 248, 373–382.
Carter, J., Viviano-Beck, C., Le Deit, L., Bishop, J.L., Loizeau, D., 2015b. Orbital detection and implications of akaganéite on Mars. Icarus 253, 296–310.
Chamley, H., 1989. Clay Sedimentology. Springer-Verlag, New York.
Chemtob, S.M., Nickerson, R.D., Morris, R.V., Agresti, D.G., Catalano, J.G., 2015. Synthesis and structural characterization of ferrous trioctahedral smectites: implications for clay mineral genesis and detectability on Mars. Journal of Geophysical Research: Planets 120, 1119–1140.
Chevrier, V., Poulet, F., Bibring, J.-P., 2007. Early geochemical environment of Mars as determined from thermodynamics of phyllosilicates. Nature 448, 60–63.
Conner, A.J., Benison, K.C., 2013. Acidophilic halophilic microorganisms in fluid inclusions in halite from Lake Magic, Western Australia. Astrobiology 13, 850–860.
Cornell, R.M., Schwertmann, U., 2003. The Iron Oxides. Structure, Properties, Reactions, Occurrences and Uses, 2nd Ed. Wiley-VCH, Weinheim.
Danielsen, J.M., Bishop, J.L., 2018. Characterization of jarosite-bearing outcrops at Mawrth Vallis, Mars. Lunar Planet. Sci. Conf. The Woodlands, TX (Abstract #1804).
Danielsen, J.M., Bishop, J.L., Usabal, G.S., Miura, J.K., Sessa, A.M., Wray, J.J., Itoh, Y., Parente, M., Murchie, S.M., 2019. Characterization of outcrops containing "doublet" spectra at Mawrth Vallis, Mars. In: 50th Lunar Planet. Sci. Conf. The Woodlands, TX. Abstract #3017.
Dong, H., Kostka, J.E., Kim, J.W., 2003. Microscopic evidence for microbial dissolution of smectite. Clay Clay Miner. 51, 502–512.
Dong, H., Jaisi, D.P., Km, J., Zhang, G., 2009. Microbe-clay mineral interactions. Am. Mineral. 94, 1505–1519.
Ehlmann, B.L., Dundar, M., 2015. Are Noachian/Hesperian acidic waters key to generating Mars' regional-scale aluminum phyllosilicates? The importance of jarosite co-occurrences with Al-phyllosilicate units. In: 46th Lunar Planet. Sci. Conf. The Woodlands, TX (Abstract #1635).
Farrand, W.H., Glotch, T.D., Rice Jr., J.W., Hurowitz, J.A., Swayze, G.A., 2009. Discovery of jarosite within the Mawrth Vallis region of Mars: implications for the geologic history of the region. Icarus 204, 478–488.
Farrand, W.H., Glotch, T.D., Horgan, B., 2014. Detection of copiapite in the northern Mawrth Vallis region of Mars: evidence of acid sulfate alteration. Icarus 241, 346–357.
Fassett, C.I., Head, J.W., 2008. Valley network-fed, open-basin lakes on Mars: distribution and implications for Noachian surface and subsurface hydrology. Icarus 198, 37–56.
Faye, G.H., 1968. The optical absorption spectra of iron in six-coordinate sites in chlorite, biotite, phlogopite and vivianite; some aspects of pleochroism in the sheet silicates. Can. Mineral. 9, 403–425.
Fialips, C.-I., Huo, D., Yan, L., Wu, J., Stucki, J.W., 2002. Effect of Fe oxidation state on the IR spectra of Garfield nontronite. Am. Mineral. 87, 630–641.
Flahaut, J., Bishop, J.L., Fueten, F., Quantin, C., Thollot, P., van Westrenen, W., Davies, G.R., 2014. New hydrated phase detections in Valles Marineris: insights into the canyon's aqueous history. In: Eighth International Conference on Mars, Pasadena, CA (Abstract #1411).
Flahaut, J., Martinet, M., Bishop, J.L., Davies, G.R., Potts, N.J., 2017. Remote sensing and in situ mineralogic survey of the Chilean salars: an analog to Mars evaporate deposits? icarus 282, 152–173.

Gates, W.P., Jaunet, A.M., Tessier, D., Cole, M.A., Wilkinson, H.T., Stucki, J.W., 1998. Swelling and texture of iron-bearing smectites reduced by bacteria. Clay Clay Miner. 46, 487–497.
Gross, C., Carter, J., Poulet, F., Loizeau, D., Bishop, J.L., Horgan, B., Michalski, J.R., 2017. Mawrth Vallis - an auspicious destination for the ESA and NASA 2020 landers. In: 48th Lunar Planet. Sci. Conf. The Woodlands, TX (Abstract #2194).
Gwinner, K., et al., 2016. The High Resolution Stereo Camera (HRSC) of Mars Express and its approach to science analysis and mapping for Mars and its satellites. Planetary and Space Science 126, 93–138.
Horgan, B., Kahlmann-Robinson, J.A., Bishop, J.L., Christensen, P.R., 2013. Climate change and a sequence of habitable ancient surface environments preserved in pedogenically altered sediments at Mawrth Vallis, Mars. In: 44th Lunar Planet. Sci. Conf. The Woodlands, TX (Abstract #3059).
Horgan, B., Rice, M.S., Farrand, W.H., Sheldon, N.D., Bishop, J.L., 2015. Possible microbial energy pathways from iron and sulfur redox gradients at mawrth vallis and gale crater, mars. AbSciCon, Chicago (Abstract #7463).
Jaisi, D.P., Dong, H., Liu, C., 2007. Influence of biogenic Fe(II) on the extent of microbial reduction of Fe(III) in clay mineral nontronite, illite, and chlorite. Geochimica Cosmochimica Acta 71, 1145–1158.
Johnson, S.S., Chevrette, M.G., Ehlmann, B.L., Benison, K.C., 2015. Insights from the metagenome of an acid salt lake: the role of biology in an extreme depositional environment. PLoS One 10, e0122869.
Johnson, S.S., Millan, M., Graham, H., Benison, K.C., Williams, A.J., McAdam, A., Knudson, C.A., Andrejkovicova, S., Achilles, C., 2020. Lipid biomarkers in ephemeral acid salt lake mudflat/sandflat sediments: implications for Mars. Astrobiology 20. https://doi.org/10.1089/ast.2017.1812 (in press).
Kirk, R.L., et al., 2008. Ultrahigh resolution topographic mapping of Mars with MRO HiRISE stereo images: meter-scale slopes of candidate Phoenix landing sites. J. Geophys. Res. 113, E00A24. https://doi.org/10.1029/2007JE003000.
Lane, M.D., Bishop, J.L., Dyar, M.D., Hiroi, T., Mertzman, S.A., Bish, D.L., King, P.L., Rogers, A.D., 2015. Mid-infrared emission spectroscopy and visible/near-infrared reflectance spectroscopy of Fe-sulfate minerals. Am. Mineral. 100, 66–82.
Lear, P.R., Stucki, J.W., 1987. Intervalence electron transfer and magnetic exchange in reduced nontronite. Clay Clay Miner. 35, 373–378.
Loizeau, D., Mangold, N., Poulet, F., Bibring, J.-P., Gendrin, A., Ansan, V., Gomez, C., Gondet, B., Langevin, Y., Masson, P., Neukum, G., 2007. Phyllosilicates in the Mawrth Vallis region of Mars. J. Geophys. Res. 112 https://doi.org/10.1029/2006JE002877.
Loizeau, D., Mangold, N., Poulet, F., Ansan, V., Hauber, E., Bibring, J.P., Gondet, B., Langevin, Y., Masson, P., Neukum, G., 2010. Stratigraphy in the Mawrth Vallis region through OMEGA, HRSC color imagery and DTM. Icarus 205, 396–418.
Loizeau, D., Carter, J., Bouley, S., Mangold, N., Poulet, F., Bibring, J.P., Costard, F., Langevin, Y., Gondet, B., Murchie, S.L., 2012a. Characterization of hydrated silicate-bearing outcrops in Tyrrhena Terra, Mars: implications to the alteration history of Mars. Icarus 219, 476–497.
Loizeau, D., Werner, S.C., Mangold, N., Bibring, J.P., Vago, J.L., 2012b. Chronology of deposition and alteration in the Mawrth Vallis region, Mars. Planetary and Space Science 72, 31–43.
Lowe, D.R., Bishop, J.L., Loizeau, D., Wray, J.J., Beyer, R.A., 2020. Deposition of >3.7 Ga clay-rich strata of the Mawrth Vallis Group, Mars, in lacustrine, alluvial, and aeolian environments. GSA Bull. 132, 17–30.
Madejová, J., Budják, J., Janek, M., Komadel, P., 1998. Comparative FT-IR study of structural modifications during acid treatment of dioctahedral smectites and hectorite. Spectrochim. Acta Part A. 54, 1397–1406.
Malin, M.C., Bell III, J.F., Cantor, B.A., Caplinger, M.A., Calvin, W.M., Clancy, R.T., Edgett, K.S., Edwards, L., Haberle, R.M., James, P.B., Lee, S.W., Ravine, M.A., Thomas, P.C., Wolff, M.J., 2007. Context camera investigation on board the Mars Reconnaissance Orbiter. J. Geophys. Res. 112, E05S04. https://doi.org/10.1029/2006JE002808.
Manceau, A., Drits, V.A., Lanson, B., Chateigner, D., Wu, J., Huo, D., Gates, W.P., Stucki, J.W., 2000. Oxidation-reduction mechanism of iron in dioctahedral smectites: II. Crystal chemistry of reduced Garfield nontronite. Am. Mineral. 85, 153–172.
McEwen, A.S., et al., 2007. Mars Reconnaissance Orbiter's High Resolution Imaging Science Experiment (HiRISE). J. Geophys. Res. 112 https://doi.org/10.1029/2005JE002605.
McEwen, A.S., et al., 2010. The High Resolution Imaging Science Experiment (HiRISE) during MRO's Primary Science Phase (PSP). Icarus 205, 2–37. https://doi.org/10.1016/j.icarus.2009.04.023.
McGuire, P.C., et al., 2009. An improvement to the volcano-scan algorithm for atmospheric correction of CRISM and OMEGA spectral data. Planetary and Space Science 57, 809–815.
McKeown, N.K., Bishop, J.L., Noe Dobrea, E.Z., Ehlmann, B.L., Parente, M., Mustard, J.F., Murchie, S.L., Swayze, G.A., Bibring, J.-P., Silver, E., 2009. Characterization of phyllosilicates observed in the central Mawrth Vallis region, Mars, their potential formational processes, and implications for past climate. J. Geophys. Res. 114 https://doi.org/10.1029/2008JE003301.
Michalski, J.R., Bleacher, J.E., 2013. Supervolcanoes within an ancient volcanic province in Arabia Terra, Mars. Nature 502, 47–52.
Michalski, J.R., Fergason, R.L., 2009. Composition and thermal inertia of the Mawrth Vallis region of Mars from TES and THEMIS data. Icarus 199, 25–48.
Michalski, J.R., Noe Dobrea, E.Z., 2007. Evidence for a sedimentary origin of clay minerals in the Mawrth Vallis region, Mars. Geology 35, 951–954.
Michalski, J.R., Poulet, F., Loizeau, D., Mangold, N., Noe Dobrea, E.Z., Bishop, J.L., Wray, J.J., McKeown, N.K., Parente, M., Hauber, E., Altieri, F., Carrozzo, F.G., Niles, P.B., 2010. The Mawrth Vallis region of Mars: a potential landing site for the Mars Science Laboratory (MSL) mission. Astrobiology 10, 687–703.
Michalski, J.R., Niles, P.B., Cuadros, J., Baldridge, A.M., 2013. Multiple working hypotheses for the formation of compositional stratigraphy on Mars: insights from the Mawrth Vallis region. Icarus 226, 816–840.
Miura, J.K., Bishop, J.L., 2018. Constraining sulfate and hydrated silica abundances on Mars with laboratory mixtures. In: AGU Fall Meeting, Washington, DC (Abstract #P31H-3811).
Morgan, F., Mustard, J.F., Wiseman, S.M., Seelos, F.P., Murchie, S.L., McGuire, P.C., CRISM Team, 2011. Improved algorithm for CRISM volcano scan atmospheric correction. In: 42nd Lunar Planet. Sci. Conf. The Woodlands, TX (Abstract #2453).
Mormile, M.R., Hong, B.-Y., Benison, K.C., 2009. Molecular analysis of the microbial communities of Mars analog lakes in Western Australia. Astrobiology 9, 919–930.
Morris, R.V., Golden, D.C., Ming, D.W., Graff, T.G., Arvidson, R.E., Wiseman, S.M., Lichtenberg, K.A., 2009. Visible and near-IR reflectance spectra for smectite, sulfate and perchlorate under dry conditions for interpretation of martian surface mineralogy. In: 40th Lunar Planet. Sci. Conf. LPI, Houston. Abstract. #2317.
Murchie, S.L., Seelos, F.P., Buczkowski, D.L., Mustard, J.F., Ehlmann, B.L., Milliken, R.E., Noe Dobrea, E., Bishop, J.L., McKeown, N.K., Wiseman, S., Arvidson, R.E., Wray, J. J., Swayze, G.A., Clark, R.N., 2009a. Diversity of Martain phyllosilicate deposits from orbital remote sensing. International Clay Conference, Castellaneta Marina, Italy.
Murchie, S.L., et al., 2009b. The Compact Reconnaissance Imaging Spectrometer for Mars investigation and data set from the Mars Reconnaissance Orbiter's primary science phase. J. Geophys. Res. 114, E00D07. https://doi.org/10.1029/2009JE003344.
Neukum, G., Jaumann, R., Hoffmann, H., Hauber, E., Head, J.W., Basilevsky, A.T., Ivanov, B.A., Werner, S.C., van Gasselt, S., Murray, J.B., McCord, T., TeamThe, H.C.-I., 2004. Recent and episodic volcanic and glacial activity on Mars revealed by the High Resolution Stereo Camera. Nature 432, 971–979.
Noe Dobrea, E.Z., et al., 2010. Mineralogy and stratigraphy of phyllosilicate-bearing and dark mantling units in the greater Mawrth Vallis/west Arabia Terra area: constraints on geological origin. J. Geophys. Res. 115 https://doi.org/10.1029/2009JE003351.
Parente, M., Saranathan, A.M., Wiseman, S.J., Ehlmann, B.L., Pan, L., 2014. Denoising CRISM images: a new look. In: 45th Lunar Planet Sci. Conf. The Woodlands, TX (Abstract # 2900).
Parfitt, R.L., 2009. Allophane and imogolite: role in soil biogeochemical processes. Clay Miner. 44, 135–155.
Pelkey, S.M., Mustard, J.F., Murchie, S., Clancy, R.T., Wolff, M., Smith, M., Milliken, R. E., Bibring, J.-P., Gendrin, A., Poulet, F., Langevin, Y., Gondet, B., 2007. CRISM multispectral summary products: parameterizing mineral diversity on Mars from reflectance. J. Geophys. Res. 112 https://doi.org/10.1029/2006JE002831.
Perrin, S., Bishop, J.L., Parker, W.G., King, S.J., Lafuente, B., 2018. Mars evaporite analog site containing jarosite and gypsum at Sulfate Hill, Painted Desert, AZ. In: 49th Lunar Planet. Sci. Conf. The Woodlands, TX (Abstract #1801).
Poulet, F., Bibring, J.-P., Mustard, J.F., Gendrin, A., Mangold, N., Langevin, Y., Arvidson, R.E., Gondet, B., Gomez, C., OMEGA, 2005. Phyllosilicates on Mars and implications for early martian climate. Nature. 438, 623–627 and the Team.
Poulet, F., Mangold, N., Loizeau, D., Bibring, J.P., Langevin, Y., Michalski, J.R., Gondet, B., 2008. Abundance of minerals in the phyllosilicate-rich units on Mars. Astron. Astrophys. 487 https://doi.org/10.1051/0004-6361:200810150 and the OMEGA Team.
Poulet, F., Gross, C., Horgan, B., Loizeau, D., Bishop, J.L., Carter, J., Orgel, C., Bibring, J. P., 2020. Mawrth Vallis, Mars: a fascinating place for future in situ exploration. Astrobiology 20. https://doi.org/10.1089/ast.2019.2074 (in press).
Rasmussen, C., Dahlgren, R.A., Southard, R.J., 2010. Basalt weathering and pedogenesis across an environmental gradient in the southern Cascade Range, California, USA. Geoderma 154, 473–485.
Roach, L.H., Mustard, J.F., Swayze, G.A., Milliken, R., Bishop, J.L., Murchie, S.L., Lichtenberg, K.A., 2010. Hydrated mineral stratigraphy of Ius Chasma, Valles Marineris. Icarus 206, 253–268.
Robbins, S.J., Achille, G.D., Hynek, B.M., 2011. The volcanic history of Mars: high-resolution crater-based studies of the calderas of 20 volcanoes. Icarus 211, 1179–1203.
Saper, L., Bishop, J.L., 2011. Reflectance spectroscopy of nontronite and ripidolite mineral mixtures in context of phyllosilicate unit composition at Mawrth Vallis. In: 42nd Lunar Planet. Sci. Conf. (Abstract #2029).
Seelos, F.P., 2011. CRISM data processing and analysis products update - calibration, correction, and visualization. In: 42nd Lunar Planet. Sci. Conf. The Woodlands, TX (Abstract #1438).
Seelos, F.P., Viviano-Beck, C.E., Morgan, M.F., Romeo, G., Aiello, J.J., Murchie, S.L., 2016. CRISM hyperspectral targeted observation PDS product sets - TERs and MTRDRs. In: 47th Lunar Planet. Sci. Conf. The Woodlands, TX (Abstract #1783).
Smith, D.E., et al., 2001. Mars Orbiter Laser Altimeter: experiment summary after the first year of global mapping of Mars. J. Geophys. Res. 106, 23,689–23,722.
Squyres, S.W., et al., 2004. In situ evidence for an ancient aqueous environment at Meridiani Planum, Mars. Science 306, 1709.
Stucki, J.W., 2006. Properties and behaviour of iron in clay minerals. In: Bergaya, G.L.F., Theng, B.G.K. (Eds.), Handbook of Clay Science. Elsevier, Amsterdam, pp. 423–476.
Stucki, J.W., Komadel, P., Wilkinson, H.T., 1987. Microbial reduction of structural iron (III) in smectites. Soil Sci. Soc. Am. J. 51, 1663–1665.
Tanaka, K.L., Skinner Jr., J.A., Hare, T.M., 2005. Geologic Map of the Northern Plains of Mars, Map 2888. U.S. Geol. Surv., Flagstaff, AZ.
Tosca, N.J., Milliken, R.E., Michel, F.M., 2008. Smectite formation on early Mars: experimental constraints. Workshop on martian Phyllosilicates: Recorders of Aqueous Processes, Paris (Abstract #7030).

Usabal, G.S., Bishop, J.L., 2018. VNIR spectral analysis of laboratory nontronite/jarosite mixtures: applications to Mawrth Vallis. In: AGU Fall Meeting, Washington, DC (Abstract #P31H-3806).

Usabal, G.S., Bishop, J.L., Danielsen, J.M., Itoh, Y., Parente, M., Seelos, F., 2019. Characterization of jarosite-bearing outcrops northwest of Mawrth Valles. In: 50th Lunar Planet. Sci. Conf. The Woodlands, TX (Abstract #2234).

Viviano-Beck, C.E., Seelos, F.P., Murchie, S.L., Kahn, e.g.,, Seelos, K.D., Taylor, H.W., Taylor, K., Ehlmann, B.L., Wisemann, S.M., Mustard, J.F., Morgan, M.F., 2014. Revised CRISM spectral parameters and summary products based on the currently detected mineral diversity on Mars. Journal of Geophysical Research: Planets 119, 2014JE004627.

Warren-Rhodes, K., et al., 2007. Searching for microbial life remotely: satellite-to-rover habitat mapping in the Atacama Desert, Chile. Journal of Geophysical Research: Biogeosciences 112. https://doi.org/10.1029/2006JG000283.

Weitz, C.M., Bishop, J.L., Thollot, P., Mangold, N., Roach, L.H., 2011. Diverse mineralogies in two troughs of Noctis Labyrinthus, Mars. Geology 39, 899–902. https://doi.org/10.1130/G32045.1.

Wierzchos, J., CÁMara, B., De Los RÍOs, A., Davila, A.F., SÁNchez Almazo, I.M., Artieda, O., Wierzchos, K., GÓMez-Silva, B., McKay, C., Ascaso, C., 2011. Microbial colonization of Ca-sulfate crusts in the hyperarid core of the Atacama Desert: implications for the search for life on Mars. Geobiology 9, 44–60.

Wray, J.J., Ehlmann, B.L., Squyres, S.W., Mustard, J.F., Kirk, R.L., 2008. Compositional stratigraphy of clay-bearing layered deposits at Mawrth Vallis, Mars. Geophys. Res. Lett. 35 https://doi.org/10.1029/2008GL034385.

Wray, J.J., Squyres, S.W., Roach, L.H., Bishop, J.L., Mustard, J.F., Noe Dobrea, E.Z., 2010. Identification of the Ca-sulfate bassanite in Mawrth Vallis, Mars. Icarus 209, 416–421.

Yant, M., Young, K.E., Rogers, A.D., McAdam, A.C., Bleacher, J.E., Bishop, J.L., Mertzman, S.A., 2017. Visible, near-infrared and mid-infrared spectral characterization of Hawaiian fumarolic alteration near Kilauea's December 1974 flow: implications for spectral discrimination of alteration environments on Mars. Am. Mineral. 103, 11–25.